Published in final edited form as:
Circ Res. 2011 January 7; 108(1): 98–112. doi:10.1161/CIRCRESAHA.110.223586.

Alternans Arrhythmias: From Cell to Heart

James N. Weiss[1,2], **Michael Nivala**[1], **Alan Garfinkel**[1,3], and **Zhilin Qu**[1]

[1] UCLA Cardiovascular Research Laboratory, Department of Medicine (Cardiology), UCLA and the David Geffen School of Medicine at UCLA, Los Angeles, CA

[2] Department of Physiology, UCLA and the David Geffen School of Medicine at UCLA, Los Angeles, CA

[3] Department of Integrative Biology and Physiology, UCLA and the David Geffen School of Medicine at UCLA, Los Angeles, CA

Abstract

The goal of systems biology is to relate events at the molecular level to more integrated scales from organelle to cell, tissue and living organism. Here we review how normal and abnormal excitation-contraction (EC) coupling properties emerge from the protein scale, where behaviors are dominated by randomness, to the cell and tissue scales, where heart has to beat with reliable regularity for a life-time. Beginning with the fundamental unit of EC coupling, the couplon where L-type Ca channels in the sarcolemmal membrane adjoin ryanodine receptors in the sarcoplasmic reticulum membrane, we show how a network of couplons with three basic properties (random activation, refractoriness, and recruitment) produces the classical physiological properties of excitation-contraction (EC) coupling and, under pathophysiological conditions, leads to Ca alternans and Ca waves. Moving to the tissue scale, we discuss how cellular Ca alternans and Ca waves promote both reentrant and focal arrhythmias in the heart. Throughout, we emphasize the qualitatively novel properties which emerge at each new scale of integration.

Keywords

Cardiac excitation-contraction coupling; ventricular arrhythmias; Ca signaling; cardiac electrophysiology; heart failure

Introduction

It is a fundamental tenet of evolutionary biology that new properties which confer a survival advantage to a species are preserved. The properties endowing the greatest advantages are qualitatively novel ones in which “the whole becomes greater than the sum of the parts.” Indeed, these “emergent” properties, which arise nonintuitively from the nonlinear interactions between the parts, are the very basis of life. Without nonlinear interactions, the most fundamental aspects of living systems, such as oscillations underlying the cell cycle and the heart beat, could not exist (since in linear systems, the whole can be no more nor less than the sum of the parts). Yet recognizing this fact as a guiding principle in biology

Address for correspondence: James N. Weiss, MD, Division of Cardiology, David Geffen School of Medicine at UCLA, Los Angeles, CA 90095, Tel: 310 825-9029, Fax: 310 206-5777, jweiss@mednet.ucla.edu.

In September 2010, the average time from submission to first decision for all original research papers submitted to *Circulation Research* was 13.1 days.

Disclosures
None.

comes at a cost–if the whole is greater than the sum of the parts, then the whole cannot be understood simply by studying the parts in isolation. This premise defines the rationale for systems biology.

The most fundamental “parts” in biological systems are the genes and proteins which they encode for. Genes and proteins have fascinating properties in their own right, but they do not, by themselves, explain the qualitatively new properties that arise as these molecules self-organize themselves, stage by stage, into the components of living systems, from supramolecular complexes to organelles to cells to tissues to organs. For example, individual proteins are dominated by stochastic behaviors, as illustrated by the random-appearing opening and closing of ion channels (Fig. 1A). However, when integrated into a cardiac myocyte, the highly irregular stochastic behavior of many ion channels produces a very regular cardiac action potential (AP), intracellular Ca (Ca_i) transient and contraction (Fig. 1B), upon which the normal heart beat depends. Each of these cellular properties is not simply the statistical average of the individual proteins, but *emerges* as a qualitatively novel behavior at the level of the cell, resulting from nonlinear interactions between many different ion channels and transporters, communicating through voltage and ion concentration gradients.

As cells coupled together to form a syncytium, the emergent properties at the level of the cell integrate to produce new emergent properties at the level of tissue. For example, when cardiac cells generating APs are electrically coupled together by gap junctions, the resulting cardiac tissue becomes an excitable medium with a qualitatively new property, traveling waves. This property plays an essential physiological role, by allowing one region in the heart, the sinoatrial node, to initiate an organized spread of the AP and Ca transient from atria to ventricles to produce a coordinated contraction. However, as an excitable medium capable of supporting wave propagation, cardiac tissue also becomes susceptible to undesirable emergent properties, such as reentry, the most common cause of lethal cardiac arrhythmias (Fig. 1C). Reentry is not a property of either proteins or isolated cardiac cells; rather, it emerges only at the level of tissue, due to the interaction of cardiac cells with each other through gap junctions.

For biomedical researchers, the challenge of developing cures for diseases is not straightforward. Our major biological toolkit consists of proteins, as the therapeutic targets for pharmacologic or genetic interventions. But proteins do not by themselves cause phenomena like reentry. The stochastic properties of proteins are separated by many scales of integration from the emergent properties, e.g. the reentrant cardiac arrhythmia, that actually kill people. If we are to find cures for diseases, then we must understand how emergent properties at each scale integrate to produce new emergent properties at the next level, systematically from gene, to protein, to organelle, to tissue, to organ, to living organism. Fortunately, systems biology approaches are advancing rapidly, providing us with unprecedented experimental and theoretical tools to tackle this imposing challenge.

In this paper, we use the heart to illustrate how the whole becomes greater than the sum of the parts as we move from the subcellular Ca cycling network of a cardiac myocyte, to the myocyte itself, and, finally, to intact cardiac tissue. We begin with the fundamental Ca release unit of cardiac excitation-contraction (EC) coupling, the couplon. We show how adjacent couplon-couplon interactions, dominated by randomness, integrate to produce the classical nonrandom physiological properties of EC coupling in the cardiac myocyte. We then illustrate how these same properties, when modified pathophysiologically, lead to Ca waves and Ca alternans. Finally, moving to the tissue scale, we show how cellular Ca alternans and Ca waves integrate to promote both reentrant and focal arrhythmias. For practical reasons, we stop here, but the story continues into new dimensions as tissue is

incorporated into the heart as an organ system, and the organ system into the living organism.

From Couplon to Cell: Subcellular EC Coupling and the Genesis of Ca Alternans

We begin by describing how both physiological and pathophysiological features of EC coupling at the cellular level arise from the subcellular couplon network, emphasizing the role of three properties of couplons: Random activation, Refractoriness and Recruitment (the 3 R's). In the adult mammalian heart, contraction relies on extracellular Ca entering the cytoplasm through voltage-gated L-type Ca channels (LCC). This Ca influx induces opening of Ca release channels called ryanodine receptors (RyR), causing them to release Ca stored in the sarcoplasmic reticulum (SR) (Fig. 2A). The amount of Ca entering the cell via LCC is relatively small compared to the amount of Ca released from the SR, so that the gain of this process, called EC coupling gain, is high. To match contractile force to varying physiological needs, it is important for SR Ca release to be graded, such that the release amplitude parallels the triggering current amplitude through LCC (I_{LCC}). In his seminal 1992 modeling paper [1], Michael Stern showed that if the SR is modeled as a single compartment, high EC coupling gain is incompatible with graded Ca release: once a small amount of Ca entry through LCC induces RyR to open, the released SR Ca will form a positive feedback loop leading to complete SR Ca release from the single pool on each beat. To produce graded Ca release, he proposed a local control model, in which LCC in the sarcolemmal membrane and RyR in the SR membrane are organized into discrete Ca release units, often called couplons (Fig. 2A). In this model, SR Ca release from each couplon is controlled by its LCC: when an LCC opens in a couplon, the localized influx of extracellular Ca into the dyadic space triggers that couplon's RyR to open, but not those of adjacent couplons. Upon membrane depolarization, the number of LCC that open thereby controls the number of couplons activated to release SR Ca. Assuming that SR Ca release in each couplon is independently controlled by its associated LCC, then the whole cell Ca transient represents the sum of however many LCC are activated by the depolarization. The local control model also accounts for Ca-induced Ca release (CICR) waves under conditions of intracellular Ca overload [1]. In this setting, Ca released from one couplon diffuses to a neighboring couplon, triggering it to release Ca, and so forth, causing a propagating Ca wave mediated by CICR, irrespective of whether LCC have opened.

Advances in subcellular Ca imaging using confocal microscopy in conjunction with fluorescent Ca indicators, originally from the Lederer laboratory [2], provided strong experimental evidence supporting the local control model. These studies directly visualized spatially localized elevations in cytoplasmic Ca, called Ca sparks, postulated to be the unitary events in cardiac EC coupling. Ca sparks can be triggered in 3 ways: 1) by opening of one or more LCC in a couplon, 2) by spontaneous openings of RyR in a couplon, or 3) by opening of RyR in a couplon in response to Ca released from neighboring couplons. We refer to the first two mechanisms as primary sparks, and the third "recruitment" mechanism of spark-induced sparks as secondary sparks. Depending on relative probabilities of primary and secondary sparks, a Ca signaling hierarchy emerges [3], ranging from Ca quarks (LCC openings which fail to trigger RyR opening in the same couplon), to primary sparks, to macrosparks (primary spark + several secondary sparks), to aborted waves (primary spark + many secondary sparks), to full waves (primary spark + very many secondary sparks) and even to self-sustaining reentrant rotors (all secondary sparks).

In Stern's original local control model, graded Ca release (Fig. 3A) was nicely reproduced by assuming that couplons were all independently controlled by their endogenous LCC. That is, he assumed that under normal physiological conditions, there was no significant cross-

talk (recruitment) between couplons, in contrast to pathophysiological Ca overloaded conditions which replicated the typical features of CICR-mediated Ca waves. However, other features of EC coupling release also require explanation. First, EC coupling gain (defined as the ratio of the initial SR Ca release flux to the flux of Ca entry via LCC [4]) is voltage-dependent, having a considerably higher gain for weak depolarizations (e.g. to −20 mV) than for strong depolarizations (e.g. +20 mV) (Fig. 3B). Second, for a constant macroscopic LCC current amplitude, the fraction of SR Ca released exhibits a steep dependence on SR Ca load (steep release-load relationship, Fig. 3C). Third, at rapid heart rates, the whole cell Ca transient begins to alternate from beat to beat in a large-small pattern (whole cell Ca alternans) [5, 6](Fig. 3D).

It is conceivable that individual couplons possess these three properties intrinsically, such that the group behavior is simply the sum of the individual couplon behavior. That is, if one could study a single couplon in isolation, its spark probability would exhibit the direct equivalencies of voltage-dependent EC coupling gain, steep release-load relationship, and also be capable of alternating between large and small releases. However, another possibility is that individual couplons do not need to possess these properties intrinsically, but rather they emerge as collective behaviors of the couplon network. The truth may lie in between, as nature embellishes successful mechanisms by adding complementary features that increase dynamic range and robustness.

Indeed, we will show that the above EC coupling features can arise naturally as emergent properties of an interactive couplon network, without presupposing that they are simple summed behavior of couplons which intrinsically embody these features. Three generic properties of the couplon network are required [7, 8]. The first two are properties of individual couplons: Random activation of couplons by their associated LCC, and Refractoriness, such that once a couplon releases Ca, its RyR become refractory to further opening for a defined time period. The third property, Recruitment, describes the interaction between couplons, i.e. the probability of spark-induced sparks (secondary sparks) mediated by Ca diffusion in the network. After briefly reviewing the current state of knowledge about the molecular basis of these 3 R's, we show how their nonlinear interactions can produce graded Ca release, voltage-dependent EC coupling gain, a steep Ca release-load relationship, whole cell Ca alternans and Ca waves, all as collective behaviors of the couplon network.

The 3 R's: Randomness

All living systems must create order out of randomness. Organisms are made of molecules, and molecular interactions are dominated by randomness, such as stochastic changes in protein conformation, chance collisions between substrates and enzymes, ions and ion channel pores, etc. Yet biological systems comprised of randomly-interacting molecules require regularity to function properly. For no organ system is this more important than the heart, which must beat reliably throughout the lifetime of an organism (approximately 2.5 billion times for the average human), in the course of which it must dynamically regulate cardiac output by more than an order of magnitude to meet varying physiological needs. How such dynamic dependability arises from the randomness of molecular interactions is a fascinating puzzle.

In the cardiac couplon network, individual LCC open randomly, but, on average, the same fraction of LCC opens during each AP, triggering the same average number of couplons to release Ca. For example, a typical ventricular myocyte contains about 20,000 couplons [9–11]. Random activation of 10,000 of these couplons can produce a very regular whole cell Ca transient, whether the same or a different set of 10,000 couplons are activated on each beat. This statistical averaging of random events provides an obvious example of how random

behavior of the LCC and RyR in individual couplons is harnessed to produce a dependable, regular response of the couplon network as a whole.

Under conditions in which the probability of a primary Ca spark is low, due to either low LCC open probability, or low probability of RyR opening in response to LCC opening (called low coupling fidelity), Ca sparks tend to occur at different locations from beat-to-beat, even though the total number of Ca sparks is relatively constant. For example, this pattern is observed when Ca sparks are elicited by voltage clamps to potentials more negative than −20 mV (due to the low LCC open probability at this voltage)[12]. It is also observed with larger depolarizations in the presence of drugs causing partial LCC or RyR blockade [13–15]. When the probability of primary Ca sparks is high, however, such as during a normal AP, Ca sparks tend to occur reliably at the same sites on each beat [11, 16], although not in all species [17].

Considering that an individual couplon typically contains 5–20 LCC and 50–200 RyR [9–11], these different patterns make sense intuitively. For example, if a couplon has 10 LCC, each with a low open probability of 0.05 (i.e. a 0.95 probability of not opening), the probability that none of the 10 LCC will open on a given depolarization is $(0.95)^{10}=0.6$, so that probability of a primary Ca spark occurring from that couplon on two consecutive beats is only 0.4. However, for the same couplon in which the open probability of LCC is 0.5 (such that the probability of not opening is also 0.5), the probability that none of the LCC will open is reduced to $(0.5)^{10}=0.001$, so that a primary Ca spark will occur from that couplon on virtually every beat. Equivalently, if the LCC open probability is high (0.5), but the probability of LCC opening activating RyR is low (e.g. 0.05), primary Ca spark probability also decreases to 0.4.

Refractoriness

RyR are the pore-forming proteins mediating SR Ca release, and co-assemble with a variety of accessory proteins which regulate their open probability and sensitivity to cytoplasmic free Ca. These accessory proteins include kinases and phosphatases which regulate RyR function through phosphorylation-dephosphorylation cycles, as well as other regulatory proteins such as FKPB12.6, triadin, junction and calsequestrin (Fig. 4A). After the RyR in a couplon open and release Ca, they inactivate and require time to recover excitability (Fig. 4B). Transition to this refractory state plays a key role in Ca spark termination, and determines how rapidly a couplon can recover excitability after it has sparked. Genetic and acquired defects which accelerate couplon recovery by shortening RyR refractory period are associated with CICR-mediated Ca waves causing delayed afterdepolarizations (DADs) and triggered arrhythmias in the settings of catecholaminergic polymorphic ventricular tachycardia (CPVT) and heart failure [18].

The molecular basis of couplon refractoriness remains controversial, but the following mechanisms have been proposed, listed in order of increasing complexity:

1. Intrinsic RyR refractory period (Fig. 4C). In this mechanism, RyR undergo conformational changes between closed, open, inactivated and refractory states [1], similar to other ligand-gated channels. After opening in response to elevated cytoplasmic free Ca, a RyR spontaneously transitions to an inactivated, refractory state, terminating the Ca spark. In the simplest model, the transitions between the conformations are sensitive to cytoplasmic free Ca, but not to SR luminal free Ca. Thus, the time course of refilling of the SR is not directly related to recovery of RyR excitability, consistent with experimental observations [19] shown in Fig. 4B.
2. Direct regulation of RyR open probability by SR luminal Ca. In this mechanism, RyR are activated by increases in cytoplasmic free Ca, but their sensitivity is also

co-regulated by a Ca-binding site in the C terminus of RyR, which senses SR luminal free [Ca] [20]. As SR luminal free [Ca] decreases, Ca dissociates from the Ca sensor, decreasing RyR open probability and terminating the Ca spark. Recovery of RyR excitability occurs when Ca rebinds to this site as the SR refills during diastole. However, to account for the slower time course of RyR recovery relative to SR refilling [19] (Fig. 4B), this mechanism also requires a time delay between Ca rebinding to the RyR cytoplasmic pore and RyR recovery.

3. Indirect regulation of RyR open probability by SR luminal Ca. In this mechanism, RyR are activated as usual by increased cytoplasmic free [Ca], but the sensitivity is coregulated by calsequestrin, through its interaction with accessory proteins such as triadin and junctin in the RyR protein complex [21] (Fig. 4A). Calsequestrin is the major Ca-buffering protein in the SR lumen. When SR luminal [Ca] is low, calsequestrin in its monomeric Ca-free form interacts with triadin-junctin-RyR complexes to inhibit RyR opening. However, as the SR luminal [Ca] increases, Ca binding causes calsequestrin monomers to dissociate from the triadin-junctin-RyR complex to form dimers and polymers, removing the inhibitory effect on RyR open probability. This mechanism has been proposed to explain Ca spark termination, since as the SR empties, calsequestrin monomers reform and bind to the triadin-junctin-RyR complex, inhibiting RyR open probability. This mechanism also accounts for recovery from inactivation, since as the SR refills with Ca during diastole, Ca rebinds to calsequestrin causing it to dissociate from the triadin-junction-RyR complexes, thereby restoring their excitability. The kinetics of calsequestrin dimerization/polymerization produce a time delay between SR refilling and RyR recovery [22], consistent with experimental findings [19].

Recruitment

In our terminology (which differs from Stern [1]), recruitment refers to the probability that a primary or secondary Ca spark triggers a secondary Ca spark from a nearby couplon (i.e. a spark-induced spark). Recruitment is mediated primarily by Ca diffusion through the cytoplasm, which allows couplons to interact with each other. Without recruitment, couplons could only exhibit primary Ca sparks, with none of the other hierarchical Ca signaling features, such as macrosparks, or aborted and full Ca waves mediated by CICR [3], which are generated as secondary spark probability increases. That is, the couplon network would no longer qualify as an excitable medium.

Recruitment probability is determined by multiple factors, including cytoplasmic free Ca, SR Ca load, the state of couplon excitability/refractoriness, structural features such as the physical diffusion distance between couplons, etc. Recruitment probability naturally increases with SR Ca load, independently of whether or not RyR are coregulated by SR luminal free Ca [20, 21]. As SR Ca content increases, the amount of Ca released by a couplon increases, thereby increasing the amount of Ca that diffuses towards nearby couplons, which increases secondary spark probability. In addition, as SR Ca load increases, free cytoplasmic free Ca also rises, bringing cytoplasmic Ca sensors of RyR closer to their activation threshold. Together, these effects account for greater fractional SR Ca release as SR Ca load increases [23].

As the factor mediating interaction between neighboring couplons, recruitment plays a particularly critical role in the emergence of collective behaviors from the couplon network, including voltage-dependent ECC gain, the steep Ca release-load relationship, Ca alternans and Ca waves, as shown below.

A Generic Model of the Couplon Network

To study how collective properties arise, we constructed a generic quasi-2D spatially-extended couplon network model [8], illustrated schematically in Fig. 2B. The model includes two parallel domains, the nonjunctional SR (NSR) and the myoplasm (Myo), coupled via SR Ca release and uptake. Each couplon in the network contains: a junctional SR (jSR) microdomain which is diffusively connected with the NSR, as represented by the flux J_{SR}; a dyadic space (DS) microdomain, which is diffusively connected with the cytoplasm, represented by the flux J_{DS}. Extracellular Ca flux (J_{LCC}) enters the dyadic space through voltage-gated LCC (5 channels per couplon), which open stochastically and are simulated by a simple Markov model [8]. Ca is released from the jSR (J_{RyR}) through its associated cluster of RyR channels (100 per couplon) into the dyadic space. The RyR open stochastically and are simulated using the Markov model by Stern et al [24] (Fig. 4C). After diffusing into the surrounding myoplasm, Ca is either extruded from the cell via the Na-Ca exchanger (J_{NCX}), or taken back up into the NSR via the SERCA pump (J_{up}). Since the Na-Ca exchanger always extrudes Ca at the resting membrane voltage, a background Ca current (J_b) was added to bring Ca into the cytoplasmic domain in order to maintain a stable Ca equilibrium state.

We deliberately represented RyR using the simple model in Fig. 4C which lacks RyR coregulation by SR luminal free [Ca]. Thus, RyR are activated by increased cytoplasmic free [Ca], after which they transition to an intrinsic inactivated state, with SR luminal [Ca] having no effect on RyR open probability. We specifically chose this model in order to investigate whether major features of cardiac EC coupling could arise as collective properties of the couplon network in the absence of RyR regulation by SR luminal [Ca].

The Graded Response and Variable ECC Gain

Using the model described above, we simulated the voltage dependence of SR Ca release. As shown in Fig. 3A, SR Ca release is graded, i.e. the cytoplasmic Ca transient increases as the current through LCC (I_{LCC}) increases, matching the experimental data. Moreover, EC coupling gain (the ratio of the initial SR Ca release flux to peak I_{LCC}) decreases from “6 to “1 as I_{LCC} becomes larger (Fig. 3B, right panel), also in agreement with experimental data (left panel).

One previously hypothesized explanation for the changing EC coupling gain is that the decreased single channel conductance of LCC (i_{LCC}) with strong depolarizations may decrease their efficiency at triggering RyR opening (i.e., reduced coupling fidelity). However, in a careful analysis of the effects of i_{LCC} on EC coupling gain, Altamirano et al [25] found no increase in coupling fidelity below 0 mV. They attributed increased EC coupling gain at negative voltages to fewer redundant openings of LCC per couplon as the open probability (P_o) of LCC decreases. That is, if only one LCC opening is sufficient to trigger Ca release from a couplon, then opening of more than one LCC per couplon increases I_{LCC} without promoting additional SR Ca release, thereby reducing EC coupling gain. Consistent with this explanation, they also found that as the number (N) of open LCC (NP_o) decreased, EC coupling gain increased. Greenstein et al.[26] demonstrated the quantitative plausibility of this mechanism using simulations of couplon populations.

However, as an excitable medium, another potential mechanism contributing to voltage-dependent EC coupling gain emerges naturally from the couplon network. For depolarizations to <0 mV, fewer LCC open to trigger primary sparks, so that more couplons are available to be recruited as secondary sparks. For depolarizations to > 0 mV, however, the high open probability of LCC causes a large number of primary sparks, leaving fewer couplons available to be recruited as secondary sparks. Thus, the ECC gain is higher for

depolarizations to <0 mV not only because of fewer LCC openings per couplon in primary sparks [25, 26], but also because each primary spark recruits multiple secondary sparks. In contrast most sparks are primary sparks for deporlzations to >0 mV. This is consistent with the observation by Altamirano et al [25] that apparent spark amplitude also increased by 20–25% when ECC gain was high, which they attributed to multiple overlapping sparks (suggesting recruitment of adjacent couplons in the same sampled voxel). The simulation in Fig. 3B demonstrates the relative contribution of this factor - EC gain at voltages < 0 mV was significantly lower when the couplons were uncoupled to prevent recruitment of secondary sparks (green circles).

At voltages >+10 mV, the primary spark rate decreases because further reduction in LCC single channel conductance decreases coupling fidelity [25]. Thus, ECC gain remains low, since Ca entry via LCC is wasted for couplons that fail to release Ca despite LCC opening. However, since failed primary sparks are still available to be activated as secondary sparks, the fraction of secondary sparks increases and ECC gain remains constant and increases even slightly at >+20 (Fig. 3B).

The Steep Release-Load Relationship

A steep dependence of fractional SR Ca release on SR Ca load [23] also emerges naturally from the couplon network (Fig. 3C), even when regulation of SR Ca release by SR luminal free [Ca] [20, 21] is absent. As SR Ca content increases and, by equilibration, also increases cytoplasmic free [Ca], the probability of both primary and secondary sparks increases (Fig. 3C). In addition, as SR load increases, the larger amount of Ca released by primary sparks increases their probability of triggering secondary sparks, amplifying total SR Ca release. Note that if the couplon network is uncoupled to prevent recruitment, the slope of the release-load curve decreases significantly.

Cellular Ca alternans

Beat-to-beat alternation in the whole cell Ca transient amplitude (Fig. 3D) causes AP duration to alternate, due the effects of the Ca transient on Ca-sensitive currents including I_{LCC} and electrogenic Na-Ca exchange. Because repolarization alternans has been linked to cardiac arrhythmias [27–29] (see below), considerable effort has gone into the search for dynamical mechanisms underlying Ca alternans. Since most models of cardiac Ca cycling are single pool models, these efforts have primarily revealed mechanisms explaining how an individual couplon can be induced to alternate. If the dynamical instability causing alternans is inherent to each individual couplon (e.g. related to its SR Ca release, uptake and leak properties [27, 30]), then whole cell Ca alternans should be accompanied by alternans in individual couplons–that is, the microscopic pattern should recapitulate the macroscopic pattern. Similarly, if alternans is due to couplon refractoriness, then as heart rate increases and 2:1 block develops in a progressively increasing fraction of couplons, individual couplons should alternate along with the whole cell Ca transient. Finally, if whole cell Ca alternans is driven by alternating SR Ca load causing CICR-mediated Ca waves on alternate beats, as described by Diaz et al [6, 31], then for the simplest case, the majority of individual couplons would also alternate on a beat-to-beat basis.

However, Diaz et al [6] found that on beats with large Ca transients, the couplon sites which initiated Ca waves varied from beat-to-beat (Fig. 5A, upper trace as reproduced from their paper). That is, the pattern of Ca release from individual couplons was dyssynchronous and irregular, dominated by the randomness of couplon activation, even though the whole cell Ca transient alternated with dependable regularity. This discrepancy between irregular couplon activation during regular whole cell Ca alternans is difficult to reconcile with any of

the aforementioned mechanisms. However, this feature arises naturally from interactions between the 3 R's in an excitable couplon network [7, 8](simulated in Fig. 5A, lower trace).

For example, suppose that in a myocyte containing 20,000 couplons, the large and small whole cell Ca transients during alternans represent Ca release from 15,000 couplons on even beats and 5,000 couplons on odd beats. A different set of individual couplons may release Ca on each even beat, as long as the total comes to 15,000, and similarly for the odd beats, as long as the total comes to 5,000. That is, the randomness factor could dominate the microscopic behavior of individual couplons, despite a highly regular summated collective behavior.

To verify this, we used both numerical simulation and a mean-field representation to show that a period-doubling bifurcation (e.g. alternans) can occur in a generic system of coupled stochastically-excitable elements (e.g. a couplon network) subject to global periodic forcing (e.g. rapid pacing) [7]. The required factors underlying this bifurcation mechanism are the 3 R's: random activation, refractoriness, and recruitment. The mechanism develops at heart rates sufficiently fast to encroach upon couplon refractoriness, as follows: random couplon activation (triggered by random LCC openings) results in a spatially random distribution of primary sparks. If the primary spark rate happens to be high in one cycle, then it will be low in the next cycle, since most of the couplons activated will remain refractory. Therefore, the couplons available for activation are not only very low in number, but also randomly and sparsely distributed among a large number of refractory couplons. Since the probability of two available couplons being nearest neighbors is low, the secondary spark rate due to recruitment is low. Conversely, if the primary spark rate is high, then most of the couplons will be recovered and available to generate primary sparks in the next cycle. The chance of two available couplons being nearest neighbors is high, and thus the secondary spark rate is also high. This is illustrated in the couplon network model in Fig. 3D. For the small Ca transients shown in the lower panels (#3, #5), the ratio of secondary to primary sparks was 328/1,909 = 0.17, whereas for the large Ca transients (#4, #6), the ratio increased to 1,949/6,411= 0.30.

In other words, during alternans, the small whole cell Ca transient is composed mostly of single, primary sparks, whereas during the large whole cell Ca transient, more macrosparks (primary + several secondary sparks) are present due to more successful recruitment. In essence, this is a more spatially localized form of the same mechanism of alternating CICR waves described experimentally by Diaz et al [6] (Fig. 5A). Due to the interaction between refractoriness and random activation, a nonlinear relationship emerges, which is key for the instability. This instability does not occur if the recovered elements are not randomly distributed.

An important corollary of this general theory of EC coupling is that the specific mechanism of couplon refractoriness is not critical for whole cell Ca alternans. Similar findings were obtained using a spatially-extended excitable couplon network model in which RyR refractoriness was regulated by SR luminal Ca (via calsequestrin polymerization [22]), as in the couplon network with an intrinsic RyR refractory period and no regulation by SR luminal free Ca. In both cases, SR Ca release during whole cell Ca alternans could also be dissociated from SR Ca load, as shown in Fig. 5B by the excellent agreement between the couplon network model [8]) (lower trace) and experimental observations from Picht et al [32] (upper trace). Whole Ca alternans could emerge from the couplon network even when SR Ca content was held constant [8].

Subcellular Ca waves and Ca altenans

It is obvious that CICR-mediated Ca waves, caused by sparks triggering spark-induced secondary sparks, require recruitment. As recruitment strength increases (e.g. by increasing the SR load in the couplon network), spark-induced secondary sparks result in a gradual transition from macrosparks to aborted waves to full waves (Fig. 6A), recapitulating the Ca signaling hierarchy [3]. Subcellular Ca rotors are also possible in the couplon network (Fig. 6B), analogous to electrical rotors in tissue, and tend to form around anatomical obstacles such as nuclei.

As discussed above, the property of recruitment, coupled with random activation and refractoriness, directly links Ca waves to Ca alternans, as shown experimentally in the case of alternating CICR-mediated Ca waves [6, 31]. In addition, Ca waves can also cause Ca alternans to become spatially discordant by resetting the phase of SR Ca release in a localized region of the cell [33]. To illustrate, suppose that during Ca alternans, a spontaneous Ca wave occurs following a small Ca transient. The SR in the region invaded by the Ca wave will then be relatively refractory when the next paced AP occurs. Therefore, SR Ca release from that region will be small, in contrast to the large SR Ca release from regions not affected by the Ca wave. The result is spatially discordant subcellular Ca alternans, which perpetuates itself on subsequent beats due to the local resetting of SR refractoriness by the initial Ca wave. Other mechanisms can also cause Ca alternans to become spatially discordant, such as subcellular heterogeneity of couplon properties [34, 35], or interactions between Ca alternans and APD alternans [36].

Summary of the Network Properties of Couplons

The major novel insight arising from this 3 R theory of EC coupling is that the couplon network, as an excitable medium, can exhibit collective, emergent properties which contribute to graded SR Ca release, voltage-dependent EC coupling gain, a steep SR release-load relationship and whole cell Ca alternans, independently of whether individual couplons possess these properties intrinsically. These arise directly from the interaction between the 3 R's: randomness, refractoriness and recruitment. One of the most striking results is that regulation of RyR by luminal SR [Ca] is not required for these collective behaviors. This is not to imply that RyR by luminal SR [Ca] does not exist or is unimportant, given the clearcut experimental evidence to the contrary [20, 21]. Rather, the collective and individual properties interact synergistically to potentiate the response, as seen in Fig. 3B & C when coupled versus uncoupled networks are compared. We speculate that evolution, recognizing the advantages of these features, developed redundant mechanisms to confer robustness and extend the dynamic performance range of the network [37]. Thus, during whole cell Ca alternans, SR Ca content is usually high before large releases and low before small releases, consistent with RyR regulation by SR luminal [Ca]. However, as shown by Picht et al. [32] (Fig.5B), this relationship can be dissociated under some conditions, implying the presence of an underlying intrinsic RyR refractoriness mechanism that is not directly regulated by luminal SR [Ca].

From Cell to Tissue: Alternans, Afterdepolarizations and Arrhythmias

In this section, we move from cell to tissue. The first task is to merge the emergent property of the cardiac AP (whose subcellular origins can likewise be built up from the nonlinear dynamics of the ion channel network) with the whole cell Ca transient, whose subcellular origins from the couplon network have been reviewed above. Once the interactions between the cardiac AP and Ca transient have been defined at the cellular level, they can then be integrated at the tissue level, producing a new set of properties. For example, the emergent property of electrical wave propagation, from sinus node to atria to atrioventricular node to

His-Purkinje system to ventricular muscle, plays a key role in timing and synchronizing contraction to achieve an efficient pumping mechanism. In addition, whereas a linear array of myocytes could only produce an inefficient shortening of the same order as that of an individual myocyte, i.e. 10–15%, the highly nonlinear geometry of the heart, embodying an "180^{o} transmural fiber rotation from endocardium to epicardium, converts this modest degree of cellular shortening into an ejection fraction exceeding 50% in the normal left ventricle.

These physiologically useful tissue properties, however, come at a cost; namely, the possibility of undesirable emergent properties, such as reentry, the most common mechanism of lethal cardiac arrhythmias. Electrical reentry is not a property of either proteins or isolated cardiac cells; rather, it emerges only at the level of tissue, due the interaction of cardiac cells with each other through gap junctions. Two factors are required to initiate reentry: a trigger, and a vulnerable tissue substrate. The trigger is typically a PVC, and tissue vulnerability is enhanced by two factors: dispersion of refractoriness promoting unidirectional conduction block, and slow conduction, allowing the area with antegrade unidirectional conduction block to recover in time for retrograde wave propagation through the same region. We discuss below how the interaction between AP and Ca cycling dynamics produces both conditions, specifically: i) how Ca alternans at the cellular level plays a key role in enhancing vulnerability at the tissue level; and ii) how Ca waves at the cellular level lead to triggers at the tissue level, completing the dual requirements for initiation of reentry [27–29].

Interactive dynamics of APD and Ca alternans at the cell level

We discussed how the collective properties of the couplon network in a cardiac cell can lead to Ca alternans, even when the voltage of the cell is clamped from beat-to-beat. However, in a paced cardiac myocyte, the AP is not generally externally controlled by a voltage clamp amplifier, but is free-running. Under these conditions, information flow between Ca_i and voltage becomes bidirectional. That is, the AP controls transmembrane Ca fluxes through voltage-sensitive LCC and electrogenic Na-Ca exchange, thereby influencing SR Caloading and consequently the Ca cycling dynamics of the couplon network. Conversely, the Ca transient generated by the couplon network feeds back on Ca-sensitive ionic currents, most notably LCC and Na-Ca exchange, which shape the AP. Thus, if a myocyte is paced rapidly enough to cause Ca alternans in the couplon network, the alternating Ca transient amplitude will cause APD to alternate secondarily [38,39].

However, APD alternans can also be primary, rather than a passive response to Ca alternans. As shown in Nolasco and Dahlen's classic 1968 study [40], APD alternans can result from steep APD restitution. APD restitution refers to the relationship between APD and the preceding diastolic interval. At rest, your heart rate typically averages 60 beats per min (bpm). During the 1,000 ms between heart beats, systole (corresponding to APD) lasts ~300 ms, leaving ~700 ms for diastole, during which the ventricles refill and coronary flow oxygenates the myocardium before the next contraction. At maximal exercise, however, heart rate can reach 200 bpm, in which case the full cardiac cycle lasts only 300 ms. For the heart to function under these conditions, it is essential for the APD to shorten, to preserve diastole for ventricular filling and coronary flow. This rate-dependent shortening of APD is called APD restitution, and can be measured by plotting APD against the preceding diastolic interval, as shown in Fig. 7A. As shown originally by Nolasco and Dahlen [40], if the slope of APD restitution is greater than one, a dynamic instability (bifurcation) can occur which causes the APD to alternate in a repeating short-long pattern. Due to the bidirectional coupling between membrane voltage and Ca_i, APD alternans due to steep APD restitution will cause the Ca transient to alternate secondarily.

This raises the important question – when the myocyte is paced under conditions in which the AP can vary freely, is the onset of APD alternans due to steep APD restitution or to Ca alternans? Experimental evidence supports the latter, since at the onset of APD alternans, the APD restitution slope is typically <1 [38, 39]. However, because the AP and Ca transient are bidirectionally coupled, both factors always jointly influence the precise heart rate threshold and amplitude of APD alternans [41]. Whereas primary Ca alternans can be demonstrated by clamping AP waveform to prevent APD from alternating, there is no completely effective means to clamp intracellular Ca to prove that APD alternans can occur in the absence of Ca alternans.

In addition, the nature of the bidirectional coupling between APD and Ca strongly influences the specific pattern of alternans. This is because whereas a longer APD generally promotes a larger Ca transient, and vice versa (called *positive* APD-Ca transient coupling), the influence of the Ca transient on APD is more complex. Ca_i causes the voltage-dependent LCC to inactivate more rapidly, which tends to shorten APD during a large Ca transient; however, Ca_i extrusion by electrogenic Na-Ca exchange, which exchanges one Ca ion for 3 Na ions, generates an inward current, which tends to prolong APD. Ca_i also affects several other ionic currents, such that the net effect of the Ca transient on APD can either prolong or shorten the APD, referred to as *positive* and *negative* Ca_i-APD coupling, respectively (Fig. 7B) [27, 41]. When Ca_i-APD coupling is positive during APD alternans, the large Ca transient is associated with the long APD, producing APD and Ca alternans which are electromechanically in-phase with each other. When Ca_i-APD coupling is negative, however, the large Ca transient is associated with a short APD, producing electromechanically out-of-phase alternans. Thus, interactions between APD-Ca_i coupling and Ca_i-APD coupling influence both the rate threshold and the pattern of electromechanical alternans, including more complex patterns such as quasiperiodicity [41]. The combination of positive APD-Ca_i coupling and negative Ca_i-APD coupling can even cause Ca alternans to become spatially discordant at the subcellular level [36] .

APD and Ca alternans at the tissue level–why is it arrhythmogenic?

APD alternans is equivalent to repolarization alternans, which can be detected clinically as electrocardiographic T wave alternans [42]. In patients with heart disease, the presence of subtle micro-volt T wave alternans on the electrocardiogram at heart rates under 110 bpm confers an increased risk of sudden cardiac death [43]. The reason why repolarization alternans is arrhythmogenic has been demonstrated both experimentally [44, 45] and theoretically [46, 47]. Since the refractory period of ventricular tissue closely parallels APD under most conditions, when APD alternates, so does tissue refractoriness. This is not strongly arrhythmogenic as long as APD alternans remains spatially uniform throughout the tissue. However, when the APD alternates, so does the DI. If the DI becomes critically short, conduction velocity (CV) slows because Na channels have not had adequate time to recover from inactivation (called CV restitution, analogous to APD restitution, Fig. 7A). Thus, during APD alternans, as the DI following the long APD progressively shortens, the next AP will conduct more slowly, causing the DI, and hence APD, to oscillate over space. At this point, *spatially concordant* APD alternans transitions to *spatially discordant* APD alternans (Fig. 7C), in which APD of the same heart beat is long in one region of the tissue, and short in an adjacent region. On the next beat, the pattern reverses. The border separating these out-of-phase regions has a constant APD from beat-to-beat, and is called a nodal line. Spatially discordant APD alternans can also be induced by a PVC [47] and heterogeneous tissue properties [48, 49].

As illustrated in Fig. 7C, spatially discordant APD alternans is strongly arrhythmogenic [27, 44, 46, 47]. Suppose that during spatially discordant alternans, a PVC occurs in the short APD region. As the PVC propagates towards the nodal line, it encounters a steep APD gradient. If

this APD gradient reaches a critical steepness, the impulse will block. Meanwhile, the impulse can propagate parallel to the nodal line, waiting for the long APD region to repolarize. The impulse then enters the long APD area from the sides, and initiates figure-eight reentry. Computer simulations have documented this scenario, even in completely homogeneous tissue [46, 47]. If the tissue is heterogeneous with respect to the development of APD alternans, a PVC is not even required. Localized conduction block can occur in the region with increased susceptibility of APD alternans, while propagation is maintained in the adjacent regions to initiate reentry. Spatially discordant APD alternans is believed to be the major mechanism by which rapid pacing induces ventricular fibrillation (VF), even in normal human hearts paced very rapidly (typically >300 bpm) [27, 44, 46, 47].

Spatially discordant APD and Ca alternans in diseased hearts

In diseased and failing hearts, EC coupling, electrical and structural remodeling all conspire to markedly reduce the heart rate threshold for repolarization alternans [27, 50], as reflected clinically by microvolt T wave alternans. In advanced heart failure, Ca (and APD) alternans can sometimes be detected in the arterial pulse at normal heart rates, known as pulsus alternans.

Dynamical analysis has shown that for the same SR Ca load, the following factors promote Ca alternans: a steeper SR Ca release-load relationship (higher gain), increased SR Ca leak, and reduced SR Ca uptake rate [30]. The interactions between these three factors are complex. For example, despite its direct dynamical effect on promoting Ca alternans, selectively increasing SR Ca leak actually suppresses alternans indirectly by decreasing SR Ca load, at which the gain of the SR Ca release-load relationship is diminished [30]. Nevertheless, the net effects of heart failure remodeling promote Ca alternans via all of three factors: phosphorylating RyR via β-adrenergic and CaMKII signaling to increase their Ca sensitivity (increasing both gain and leak) as well as downregulating SERCA expression (reducing SR Ca uptake rate) [18, 51], consistent with recent evidence that repolarization alternans in human heart failure is predominantly caused by altered Ca cycling [52, 53]. How these molecular changes alter the susceptibility of the couplon network to Ca alternans (promoting electrophysiological dispersion) and Ca waves (promoting triggers), in relation to the 3 R theory, will be an interesting area to explore.

In addition, heart failure reduces repolarization reserve and upregulates eletrogenic Na-Ca exchange [54]. These changes serve to enhance the influence of the Ca transient on APD via positive Ca_i-APD coupling, and hence increase the amplitude of APD alternans (and dispersion of refractoriness) during Ca alternans. Finally, structural remodeling during heart failure is associated with both fibrosis and reduced gap junction conductance, which have also been shown to lower the threshold for spatially discordant alternans [48, 49]. By increasing the susceptibility of the failing heart to spatially discordant APD alternans, these factors may play an important role in promoting exercise-induced arrhythmias in the setting of heart failure, particularly since rapid heart rates also promote afterdepolarizations causing PVCs (see below).

Spatially discordant APD alternans may also be an important proarrhythmic factor in ischemic heart disease, even in the absence of heart failure. After an infarct, electrical remodeling of the surviving border zone tissue alters Na channel properties in a manner which slows their recovery from inactivation, causing CV to vary over a wider range of diastolic intervals. Coupled with fibrosis and gap junction remodeling [48, 49], these changes promote spatially discordant alternans. In the CAST clinical trial [55], patients who had suffered a myocardial infarction more than six months prior were treated with Na channel blocking drugs (encainide, flecainide or ethmozin). If one of these drugs was effective at suppressing PVCs by >80% and nonsustained VT by >90%, then patients were randomized

to the drug or a placebo. The surprising finding was that patients on the drug had nearly double the mortality rate compared to the placebo group. The implication is that although the number of potential triggered events (PVCs) had been reduced by more than 5-fold, the drugs must have increased the vulnerability to those PVCs by approximately 10-fold. What could do this? One possibility relates to the propensity of Na channel blockers to promote spatially discordant APD alternans. Na channel blocking drugs not only block the Na current, which slows CV, but they also delay Na channel recovery from inactivation [56], especially in chronically ischemic tissue. Thus, a longer DI is required for full Na current recovery, which broadens the range of heart rates over which CV restitution occurs. Since CV restitution plays a key role in converting spatially concordant to spatially discordant APD alternans, this factor may have significantly enhanced the tissue vulnerability to PVCs, offsetting the reduced PVC frequency.

Ca waves, delayed afterdepolarizations (DADs) and PVCs at the cell level

Although dispersion of refractoriness generated by spatially discordant APD and Ca alternans increases tissue vulnerability, initiation of reentry also requires a critically-timed PVC, as illustrated in Fig. 7C. What causes the critically-timed PVC? By increasing SR Ca loading, the rapid heart rates that promote spatially discordant APD and Caalternans also increase the probability of spontaneous CICR-mediated Ca waves in myocytes. Due to the bidirectional coupling between Ca and membrane voltage, a diastolic Ca wave depolarizes diastolic membrane voltage by activating inward Na-Ca exchange current and Ca-activated nonselective cation currents. If the resulting depolarization, called a DAD, is sufficient to reach the Na current excitation threshold, then the DAD can trigger an AP (Fig. 8A). Thus, as fast heart rates promote spatially discordant APD alternans, they simultaneously promote DADs and PVCs, resulting in the highly arrhythmogenic trigger-substrate combination shown in Fig. 7C.

Neurohumoral activation during heart failure promotes spontaneous Ca waves, by increasing Ca sensitivity of RyR via β-adrenergic [18] and CaMKII-mediated phosphorylation [51]. Couplon spacing is also decreased in heart failure [57], enhancing the recruitment probability for secondary sparks and CICR. In addition, electrical remodeling in heart failure results in a larger DAD for the same Ca wave amplitude, as a result of the upregulation in Na-Ca exchange current and downregulation of inward rectifier K current (I_{K1}) [54]. These changes increase the "diastolic Ca-voltage coupling gain" [58], enhancing the likelihood that spontaneous Ca waves will cause large enough DAD to trigger a PVC.

DADs also play a major role in catecholaminergic polymorphic ventricular tachycardia (CPVT) [18]. In this syndrome, mutations in ryanodine receptors or associated regulatory proteins such as calsequestrin lead to leakiness and accelerated recovery of SR Ca release units, enhancing both primary and secondary spark probability as SR Ca load increases [59] to promote spontaneous Ca waves and DADs [60]. High catecholamine states promote CPVT by enhancing SR Ca loading. Thus, the pathophysiology of this rare familial heart disease and common everyday heart failure share important similarities in predisposing these patients to VT/VF and sudden cardiac death.

Ca waves, DADs and PVCs at the tissue level: Overcoming the source-sink mismatch

In ventricular muscle, each myocyte is coupled to an average of 11 other myocytes by gap junctions [61, 62]. If a Ca wave occurs in a single myocyte, the source-sink mismatch is normally too great to cause a DAD. That is, once the affected myocyte tries to depolarize in response to the inward Na-Ca exchange current generated by its Ca wave, the resulting voltage difference with the surrounding normal myocytes will cause current to flow through gap junctions into the affected myocyte, suppressing the depolarization. Only when enough

myocytes in a region larger than the electrical space constant all develop Ca waves synchronously will their summated Na-Ca exchange current be sufficient to generate a DAD in tissue. This has been demonstrated in intact tissue using confocal microscopy [63]. After termination of rapid pacing, synchronous Ca waves occurring in multiple adjacent myocytes were associated with DADs. In contrast, during slow pacing, sporadic Ca waves in single myocytes did not elicit detectable DADs.

We recently performed simulations in 1D, 2D and 3D cardiac tissue to estimate how many contiguous myocytes are required to simultaneously develop a Ca wave in order to produce a DAD large enough to trigger a PVC [64]. We simulated a myocyte which the Ca wave produced an integrated Ca transient with a sufficient rate of rise and amplitude to trigger an AP when uncoupled from other cells. When these Ca wave-generating myocytes were coupled together in tissue and surrounded by normal myocytes without Ca waves, the number of contiguous myocytes with Ca waves required to produce a PVC was 80 for a 1D cable, 7,854 for 2D tissue and 817,280 for 3D tissue [64]. The latter estimate for 3D tissue agrees well with experimental data for the number of pacemaker cells required to generate a biological pacemaker [65]. Factors relevant to heart failure, such as electrical remodeling, reduced gap junction conductance, and fibrosis decreased these numbers significantly (to as low as 10 contiguous myocytes for a 1D cable, and 40 contiguous myocytes for 2D tissue). Even so, the numbers are large enough to indicate that the source-sink mismatch in intact tissue is a powerful mechanism which prevents unsynchronized Ca waves from triggering PVCs. For example, if the probability that an individual myocyte will have a Ca wave is 0.5, then the probability that 10 contiguous myocytes will all have a Ca wave after the same beat is $(0.5)^{10}$=0.00001. For this probability to reach 0.5 requires a probability for individual myocytes of 0.94. Moreover, the number of myocytes with Ca waves required to trigger a PVC increases exponentially with tissue dimension. This may account for the greater proclivity of DADs to arise from the His-Purkinje system (a network of quasi-1D cables) than from working 3D myocardium, whether or not intrinsic cellular differences between ventricular myocytes and Purkinje cells make the latter more susceptible to DADs [58].

These estimates imply that to develop a DAD of sufficient rate-of-rise and amplitude to trigger a PVC, a mechanism must exist that synchronizes Ca waves in contiguous myocytes. The nature of this synchronization mechanism is still a matter of speculation. However, we recently identified a synchronization mechanism for early afterdepolarizations (EADs) that may also be relevant to DADs. In tissue, EADs exhibit all-or-none behavior. That is, that when the fraction of contiguous EAD-generating myocytes in a given region exceeds a critical threshold, all of the cells in the tissue will have an EAD, and when the fraction is below this level, none of the cells will exhibit an EAD [64, 66, 67]. Thus, if the fraction of EAD-generating versus non-EAD-generating myocytes in two adjacent regions are randomly above and below this threshold, an EAD will occur in one region, but not the other, potentially allowing the EAD to propagate into the repolarized region to generate a PVC and initiate reentry.

DADs may behave similarly [64], since the ability of a DAD to trigger a PVC is also an all-or-none phenomenon, depending critically on whether the DAD's rate of rise and amplitude is sufficient to trigger an AP. Thus, if the fraction of myocytes with Ca waves in a given region exceeds the critical threshold allowing the resulting DAD to trigger an AP, a PVC will occur, which may then propagate into adjacent regions in which the fraction of myocytes with Ca waves is below this threshold. Moreover, as shown in Fig. 8B, subthreshold DADs influence APD. In tissue, this can result in locally altered refractoriness in the regions with Ca waves inducing subthreshold DADs, amplifying global dispersion of refractoriness. By this mechanism, Ca waves may enhance substrate vulnerability while simultaneously generating focal PVC triggers, analgous to EADs [66].

Summary and Conclusions

In this review, we have presented a theory of cardiac EC coupling which relates the properties of the couplon network at the subcellular scale to normal and abnormal EC coupling at the cell scale, and in turn to Ca-cycling mediated arrhythmogenesis at the tissue scale. In transitioning from subcellular to cell to tissue, we have emphasized how qualitatively novel emergent properties arise from the collective behavior of the "parts", such that "the whole becomes greater than the sum of the parts" at each new scale. For example, from the subcellular to cell scale, we have shown how three generic properties of the couplon network, randomness, refractoriness and recruitment (the 3 R's) operate to contribute to the normal features of cardiac EC coupling (graded release, voltage-dependent EC coupling gain, and a steep SR release-load relationship), as well as pathophysiological features such as Ca transient alternans and Ca waves at the cell level. In the process, we show how randomness-dominated events at the microscopic level integrate to produce reliable regularity at the cell level, as, for example, in the experimentally-testable prediction that macroscopic alternans of the cell's Ca transient is not necessarily accompanied by microscopic Ca alternans at the level of individual couplons.

We emphasize that the 3 R theory is based on generic properties of couplons, and neither assumes, nor is dependent upon, the specific molecular mechanisms underlying the 3 R's. Therefore, the conclusions have a generality that can accommodate a wide range of specific underlying molecular mechanisms (such as regulation of couplon refractoriness by either an intrinsic mechanism or by SR luminal Ca). This is not to imply that the molecular details are unimportant–in contrast, understanding the molecular mechanisms is critical for both further testing the validity of the theory, and using the theory as a tool to design therapeutic strategies. The most important role of the general theory is to provide a framework for analyzing how specific molecular interventions affect the properties of the integrated system at higher scales of organization, which are very difficult to predict based on intuition alone.

Moving from the cell to the tissue brings a whole new set of emergent properties into the picture, which arise as excitable cells interact with each other through gap junction coupling. Thus, from cellular excitability emerges wave propagation at the tissue level, conferring essential physiological properties underlying the coordination of the normal heart beat. However, wave propagation also imparts pathophysiological consequences, such as spatially discordant APD alternans, DADs, and focal and reentrant cardiac arrhythmias that can lead to sudden cardiac death by the mechanisms described above.

By using this multistage systems approach to link subcellular properties to cellular and then tissue level phenomena, our goal is to create a framework relating molecular properties of proteins to tissue level behaviors such as arrhythmias that actually kill people. Once this is completed, it remains to link the tissue behaviors to those of the organ system as a whole, and, finally, to the living organism. With this framework, we can begin to systematically examine how pharmacologic or genetic manipulations targeting key proteins regulating the 3R's at the level of the couplon network affect the triggers and substrate vulnerability of cardiac tissue, towards the goal of suppressing arrhythmias without disturbing normal EC coupling.

Acknowledgments

Sources of Funding

Supported by NIH/NHLBI grants P01 HL078931, R01 HL103662 and the Laubisch and Kawata Endowments.

Nonstandard Abbreviations and Acronyms

AP	action potential
APD	AP duration
DAD	delayed afterdepolarization
EAD	early afterdepolarization
EC	excitation-contraction
LCC	L-type Ca channel
PVC	premature ventricular complex
RyR	ryanodine receptor
SR	sarcoplasmic reticulum

References

1. Stern MD. Theory of excitation-contraction coupling in cardiac muscle. Biophys J. 1992; 63(2): 497–517. [PubMed: 1330031]
2. Cheng H, Lederer WJ, Cannell MB. Calcium sparks: elementary events underlying excitation-contraction coupling in heart muscle. Science. 1993; 262(5134):740–744. [PubMed: 8235594]
3. Lipp P, Niggli E. A hierarchical concept of cellular and subcellular Ca(2+)-signalling. Progress in Biophysics and Molecular Biology. 1996; 65(3):265–296. [PubMed: 9062435]
4. Wier WG, Egan TM, Lopez-Lopez JR, Balke CW. Local control of excitation-contraction coupling in rat heart cells. J Physiol. 1994; 474(3):463–471. [PubMed: 8014907]
5. Eisner DA, Diaz ME, Li Y, O'Neill SC, Trafford AW. Stability and instability of regulation of intracellular calcium. Exp Physiol. 2005; 90(1):3–12. [PubMed: 15572459]
6. Diaz ME, O'Neill SC, Eisner DA. Sarcoplasmic reticulum calcium content fluctuation is the key to cardiac alternans. Circ Res. 2004; 94(5):650–656. [PubMed: 14752033]
7. Cui X, Rovetti RJ, Yang L, Garfinkel A, Weiss JN, Qu Z. Period-doubling bifurcation in an array of coupled stochastically excitable elements subjected to global periodic forcing. Phys Rev Lett. 2009; 103(4):044102. [PubMed: 19659359]
8. Rovetti R, Cui X, Garfinkel A, Weiss JN, Qu Z. Spark-induced sparks as a mechanism of intracellular calcium alternans in cardiac myocytes. Circ Res. 2010; 106(10):1582–1591. [PubMed: 20378857]
9. Franzini-Armstrong C, Protasi F, Ramesh V. Shape, size, and distribution of Ca(2+) release units and couplons in skeletal and cardiac muscles. Biophys J. 1999; 77(3):1528–1539. [PubMed: 10465763]
10. Bers DM, Stiffel VM. Ratio of ryanodine to dihydropyridine receptors in cardiac and skeletal muscle and implications for E-C coupling. Am J Physiol. 1993; 264(6 Pt 1):C1587–1593. [PubMed: 8333507]
11. Inoue M, Bridge JHB. Variability in couplon size in rabbit ventricular myocytes. Biophys J. 2005; 89(5):3102–3110. [PubMed: 16113111]
12. Cannell MB, Cheng H, Lederer WJ. The control of calcium release in heart muscle. Science. 1995; 268:1045–1049. [PubMed: 7754384]
13. Lopez-Lopez JR, Shacklock PS, Balke CW, Wier WG. Local calcium transients triggered by single L-type calcium channel currents in cardiac cells. Science. 1995; 268(5213):1042–1045. [PubMed: 7754383]
14. Cheng H, Cannell MB, Lederer WJ. Partial inhibition of Ca2+ current by methoxyverapamil (D600) reveals spatial nonuniformities in [Ca2+]i during excitation-contraction coupling in cardiac myocytes. Circ Res. 1995; 76(2):236–241. [PubMed: 7834834]

15. Cheng H, Cannell MB, Lederer WJ. Partial inhibition of Ca2+ current by methoxyverapamil (D600) reveals spatial nonuniformities in [Ca2+](i) during excitation- contraction coupling in cardiac myocytes. Circ Res. 1995; 76:236–241. [PubMed: 7834834]
16. Inoue M, Bridge JH. Ca2+ sparks in rabbit ventricular myocytes evoked by action potentials: involvement of clusters of L-type Ca2+ channels. Circ Res. 2003; 92(5):532–538. [PubMed: 12609971]
17. Bridge JH, Ershler PR, Cannell MB. Properties of Ca2+ sparks evoked by action potentials in mouse ventricular myocytes. J Physiol. 1999; 518 (Pt 2):469–478. [PubMed: 10381593]
18. Wehrens XH, Lehnart SE, Marks AR. Intracellular calcium release and cardiac disease. Annu Rev Physiol. 2005; 67:69–98. [PubMed: 15709953]
19. Brochet DX, Yang D, Di Maio A, Lederer WJ, Franzini-Armstrong C, Cheng H. Ca2+ blinks: rapid nanoscopic store calcium signaling. Proc Natl Acad Sci U S A. 2005; 102(8):3099–3104. [PubMed: 15710901]
20. Jiang D, Xiao B, Yang D, Wang R, Choi P, Zhang L, Cheng H, Chen SR. RyR2 mutations linked to ventricular tachycardia and sudden death reduce the threshold for store-overload-induced Ca2+ release (SOICR). Proc Natl Acad Sci U S A. 2004; 101(35):13062–13067. [PubMed: 15322274]
21. Gyorke I, Hester N, Jones LR, Gyorke S. The role of calsequestrin, triadin, and junctin in conferring cardiac ryanodine receptor responsiveness to luminal calcium. Biophys J. 2004; 86(4): 2121–2128. [PubMed: 15041652]
22. Restrepo JG, Weiss JN, Karma A. Calsequestrin-mediated mechanism for cellular calcium transient alternans. Biophys J. 2008; 95(8):3767–3789. [PubMed: 18676655]
23. Shannon TR, Ginsburg KS, Bers DM. Potentiation of fractional sarcoplasmic reticulum calcium release by total and free intra-sarcoplasmic reticulum calcium concentration. Biophys J. 2000; 78(1):334–343. [PubMed: 10620297]
24. Stern MD, Song LS, Cheng H, Sham JS, Yang HT, Boheler KR, Rios E. Local control models of cardiac excitation-contraction coupling. A possible role for allosteric interactions between ryanodine receptors. J Gen Physiol. 1999; 113(3):469–489. [PubMed: 10051521]
25. Altamirano J, Bers DM. Voltage dependence of cardiac excitation contraction coupling: Unitary Ca current amplitude and open channel probability. Circ Res. 2007; 101(6):590–597. [PubMed: 17641229]
26. Greenstein JL, Hinch R, Winslow RL. Mechanisms of excitation-contraction coupling in an integrative model of the cardiac ventricular myocyte. Biophys J. 2006; 90(1):77–91. [PubMed: 16214852]
27. Weiss JN, Karma A, Shiferaw Y, Chen PS, Garfinkel A, Qu Z. From pulsus to pulseless: the saga of cardiac alternans. Circ Res. 2006; 98(10):1244–1253. [PubMed: 16728670]
28. Eisner DA, Li Y, O'Neill SC. Alternans of intracellular calcium: mechanism and significance. Heart Rhythm. 2006; 3(6):743–745. [PubMed: 16731482]
29. Laurita KR, Rosenbaum DS. Cellular mechanisms of arrhythmogenic cardiac alternans. Prog Biophys Mol Biol. 2008; 97(2–3):332–347. [PubMed: 18395246]
30. Xie LH, Sato D, Garfinkel A, Qu Z, Weiss JN. Intracellular Ca alternans: coordinated regulation by sarcoplasmic reticulum release, uptake, and leak. Biophys J. 2008; 95(6):3100–3110. [PubMed: 18539635]
31. Diaz ME, Eisner DA, O'Neill SC. Depressed ryanodine receptor activity increases variability and duration of the systolic Ca2+ transient in rat ventricular myocytes. Circ Res. 2002; 91(7):585–593. [PubMed: 12364386]
32. Picht E, Desantiago J, Blatter LA, Bers DM. Cardiac alternans do not rely on diastolic sarcoplasmic reticulum calcium content fluctuations. Circ Res. 2006; 99(7):740–748. [PubMed: 16946134]
33. Xie LH, Weiss JN. Arrhythmogenic consequences of intracellular calcium waves. Am J Physiol Heart Circ Physiol. 2009; 297(3):H997–H1002. [PubMed: 19561309]
34. Aistrup GL, Kelly JE, Kapur S, Kowalczyk M, Sysman-Wolpin I, Kadish AH, Wasserstrom JA. Pacing-induced heterogeneities in intracellular Ca2+ signaling, cardiac alternans, and ventricular arrhythmias in intact rat heart. Circ Res. 2006; 99(7):e65–73. [PubMed: 16960102]

35. Aistrup GL, Shiferaw Y, Kapur S, Kadish AH, Wasserstrom JA. Mechanisms underlying the formation and dynamics of subcellular calcium alternans in the intact rat heart. Circ Res. 2009; 104(5):639–649. [PubMed: 19150887]
36. Shiferaw Y, Karma A. Turing instability mediated by voltage and calcium diffusion in paced cardiac cells. Proc Natl Acad Sci U S A. 2006; 103(15):5670–5675. [PubMed: 16574775]
37. Lusis AJ, Weiss JN. Cardiovascular networks: systems-based approaches to cardiovascular disease. Circulation. 2010; 121(1):157–170. [PubMed: 20048233]
38. Pruvot E, Katra RP, Rosenbaum DS, Laurita KR. Calcium cycling as mechanism of repolarization alternans onset in the intact heart. Circulation. 2002; 106(19):191–192. [PubMed: 12105157]
39. Goldhaber JI, Xie LH, Duong T, Motter C, Khuu K, Weiss JN. Action potential duration restitution and alternans in rabbit ventricular myocytes: the key role of intracellular calcium cycling. Circ Res. 2005; 96(4):459–466. [PubMed: 15662034]
40. Nolasco JB, Dahlen RW. A graphic method for the study of alternation in cardiac action potentials. J Appl Physiol. 1968; 25:191–196. [PubMed: 5666097]
41. Shiferaw Y, Sato D, Karma A. Coupled dynamics of voltage and calcium in paced cardiac cells. Physical Review E (Statistical, Nonlinear, and Soft Matter Physics). 2005; 71(2):021903.
42. Rosenbaum DS. T wave alternans: a mechanism of arrhythmogenesis comes of age after 100 years. J Cardiovasc Electrophysiol. 2001; 12(2):207–209. [PubMed: 11232620]
43. Rosenbaum DS, Jackson LE, Smith JM, Garan H, Ruskin JN, Cohen RJ. Electrical alternans and vulnerability to ventricular arrhythmias. N Engl J Med. 1994; 330(4):235–241. [PubMed: 8272084]
44. Pastore JM, Girouard SD, Laurita KR, Akar FG, Rosenbaum DS. Mechanism linking T-wave alternans to the genesis of cardiac fibrillation. Circulation. 1999; 99(10):1385–1394. [PubMed: 10077525]
45. Cao JM, Qu Z, Kim YH, Wu TJ, Garfinkel A, Weiss JN, Karagueuzian HS, Chen PS. Spatiotemporal heterogeneity in the induction of ventricular fibrillation by rapid pacing: importance of cardiac restitution properties. Circ Res. 1999; 84(11):1318–1331. [PubMed: 10364570]
46. Qu ZL, Garfinkel A, Chen PS, Weiss JN. Mechanisms of discordant alternans and induction of reentry in simulated cardiac tissue. Circulation. 2000; 102(14):1664–1670. [PubMed: 11015345]
47. Watanabe MA, Fenton FH, Evans SJ, Hastings HM, Karma A. Mechanisms for discordant alternans. Journal of Cardiovascular Electrophysiology. 2001; 12(2):196–206. [PubMed: 11232619]
48. Pastore JM, Laurita KR, Rosenbaum DS. Importance of spatiotemporal heterogeneity of cellular restitution in mechanism of arrhythmogenic discordant alternans. Heart Rhythm. 2006; 3(6):711–719. [PubMed: 16731476]
49. Pastore JM, Rosenbaum DS. Role of structural barriers in the mechanism of alternans-induced reentry. Circ Res. 2000; 87(12):1157–1163. [PubMed: 11110773]
50. Wilson LD, Jeyaraj D, Wan X, Hoeker GS, Said TH, Gittinger M, Laurita KR, Rosenbaum DS. Heart failure enhances susceptibility to arrhythmogenic cardiac alternans. Heart Rhythm. 2009; 6(2):251–259. [PubMed: 19187920]
51. Curran J, Hinton MJ, Rios E, Bers DM, Shannon TR. Beta-adrenergic enhancement of sarcoplasmic reticulum calcium leak in cardiac myocytes is mediated by calcium/calmodulin-dependent protein kinase. Circ Res. 2007; 100(3):391–398. [PubMed: 17234966]
52. Narayan SM, Bayer JD, Lalani G, Trayanova NA. Action potential dynamics explain arrhythmic vulnerability in human heart failure: a clinical and modeling study implicating abnormal calcium handling. J Am Coll Cardiol. 2008; 52(22):1782–1792. [PubMed: 19022157]
53. Bayer JD, Narayan SM, Lalani GG, Trayanova NA. Rate-dependent action potential alternans in human heart failure implicates abnormal intracellular calcium handling. Heart Rhythm. 2010; 7(8): 1093–1101. [PubMed: 20382266]
54. Shannon TR, Wang F, Bers DM. Regulation of cardiac sarcoplasmic reticulum Ca release by luminal [Ca] and altered gating assessed with a mathematical model. Biophys J. 2005; 89(6): 4096–4110. [PubMed: 16169970]

55. Moss AJ. Investigators CASTC. Effect of encainide and flecainide on mortality in a random trial of arrhythmia suppression after myocardia infarction. N Engl J Med. 1989; 321:406–412. [PubMed: 2473403]
56. Pu J, Balser JR, Boyden PA. Lidocaine action on Na+ currents in ventricular myocytes from the epicardial border zone of the infarcted heart. Circ Res. 1998; 83(4):431–440. [PubMed: 9721700]
57. Chen-Izu Y, Ward CW, Stark W Jr, Banyasz T, Sumandea MP, Balke CW, Izu LT, Wehrens XH. Phosphorylation of RyR2 and shortening of RyR2 cluster spacing in spontaneously hypertensive rat with heart failure. Am J Physiol Heart Circ Physiol. 2007; 293(4):H2409–2417. [PubMed: 17630346]
58. Maruyama M, Joung B, Tang L, Shinohara T, On YK, Han S, Choi EK, Kim DH, Shen MJ, Weiss JN, Lin SF, Chen PS. Diastolic intracellular calcium-membrane voltage coupling gain and postshock arrhythmias: role of purkinje fibers and triggered activity. Circ Res. 2010; 106(2):399–408. [PubMed: 19926871]
59. Terentyev D, Kubalova Z, Valle G, Nori A, Vedamoorthyrao S, Terentyeva R, Viatchenko-Karpinski S, Bers DM, Williams SC, Volpe P, Gyorke S. Modulation of SR Ca release by luminal Ca and calsequestrin in cardiac myocytes: effects of CASQ2 mutations linked to sudden cardiac death. Biophys J. 2008; 95(4):2037–2048. [PubMed: 18469084]
60. Chen W, Wasserstrom JA, Shiferaw Y. Role of coupled gating between cardiac ryanodine receptors in the genesis of triggered arrhythmias. Am J Physiol Heart Circ Physiol. 2009; 297(1):H171–180. [PubMed: 19429830]
61. Hoyt RH, Cohen ML, Saffitz JE. Distribution and three-dimensional structure of intercellular junctions in canine myocardium. Circ Res. 1989; 64(3):563–574. [PubMed: 2645060]
62. Peters NS, Wit AL. Myocardial architecture and ventricular arrhythmogenesis. Circulation. 1998; 97(17):1746–1754. [PubMed: 9591770]
63. Fujiwara K, Tanaka H, Mani H, Nakagami T, Takamatsu T. Burst emergence of intracellular Ca2+ waves evokes arrhythmogenic oscillatory depolarization via the Na+-Ca2+ exchanger: simultaneous confocal recording of membrane potential and intracellular Ca2+ in the heart. Circ Res. 2008; 103(5):509–518. [PubMed: 18635824]
64. Xie Y, Sato D, Garfinkel A, Qu Z, Weiss JN. So little source, so much sink: requirements for afterdepolarizations to propagate in tissue. Biophys J. 2010; 99(5):1408–1415. [PubMed: 20816052]
65. Plotnikov AN, Shlapakova I, Szabolcs MJ, Danilo P Jr, Lorell BH, Potapova IA, Lu Z, Rosen AB, Mathias RT, Brink PR, Robinson RB, Cohen IS, Rosen MR. Xenografted adult human mesenchymal stem cells provide a platform for sustained biological pacemaker function in canine heart. Circulation. 2007; 116(7):706–713. [PubMed: 17646577]
66. Sato D, Xie LH, Sovari AA, Tran DX, Morita N, Xie F, Karagueuzian H, Garfinkel A, Weiss JN, Qu Z. Synchronization of chaotic early afterdepolarizations in the genesis of cardiac arrhythmias. Proc Natl Acad Sci U S A. 2009
67. Weiss JN, Garfinkel A, Karagueuzian HS, Chen PS, Qu Z. Early afterdepolarizations and cardiac arrhythmias. Heart Rhythm. 2010 In press.

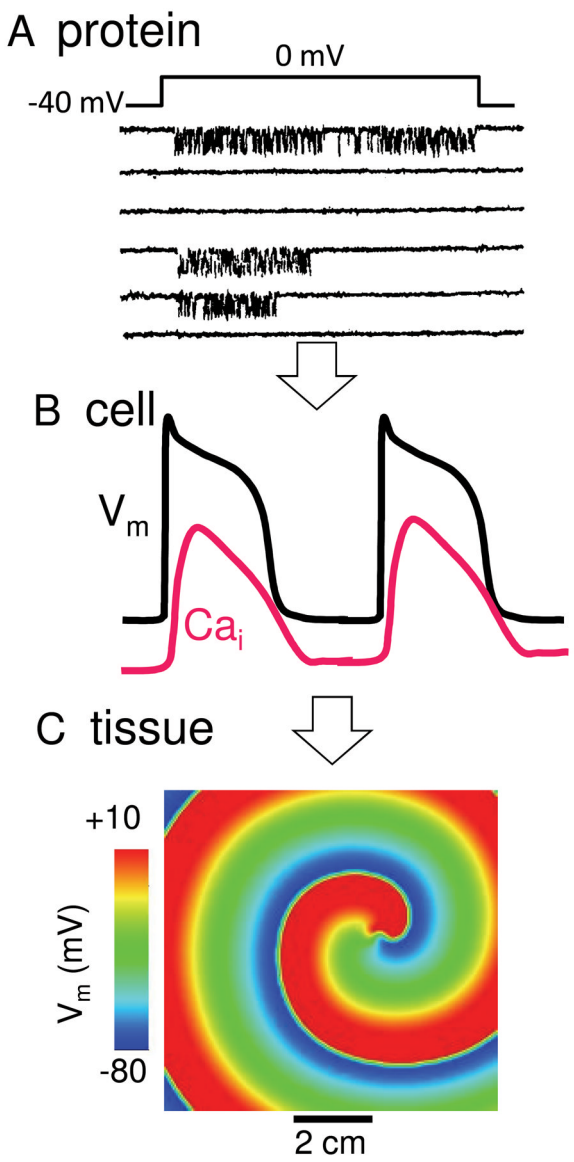

Fig. 1.

A. Stochastic protein behavior. Single channel recording of an L-type Ca channel from a cardiac myocyte, during successive voltage clamp pulses from −40 to 0 mV, showing different behaviors on each sweep. Downward deflections indicate channel openings. **B. Regular cell behavior.** Integrated behavior of stochastic ion channel network creates a dependably regular AP and Ca transient from beat-to-beat. **C. Pathological tissue behavior.** In addition to coordinating the normal heart beat, wave propagation at the tissue level also permits reentry which can cause life-threatening arrhythmias.

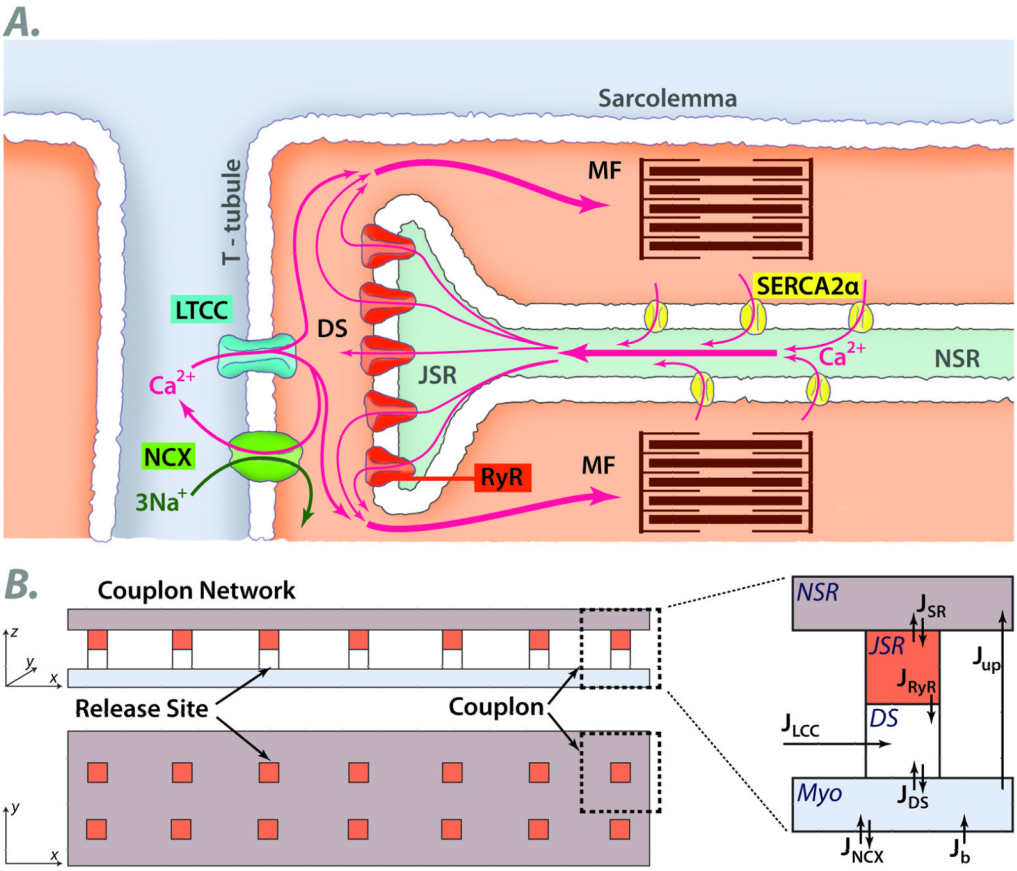

Fig. 2.

A. Schematic of a cardiac couplon, formed by L-type Ca channels (LTCC) in the T-tubular membrane and ryanodine receptors (RyR) in the apposed junctional SR (JSR). Extracellular Ca entering through LTCC triggers RyR to open, releasing SR Ca into the myoplasm (MYO) to activate the myofilaments (MF). Ca is then pumped back into the nonjuctional SR (NSR) by a Ca pump (SERCA2a) or extruded from the cell via Na-Ca exchange (NCX). **B. Spatially-distributed 2D model of the couplon network.** See text. DS=dyadic space. *J*=Ca fluxes between compartments.

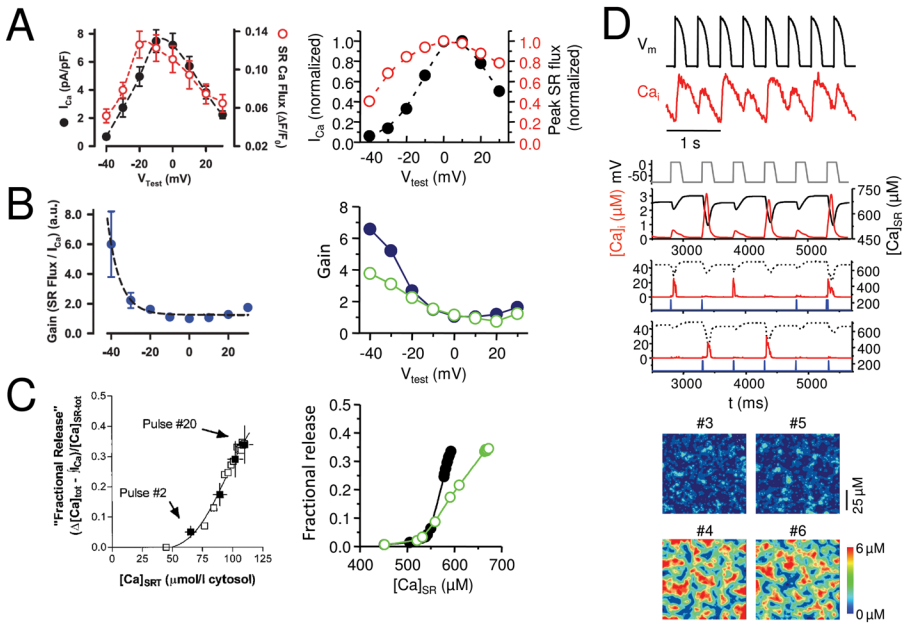

Fig. 3.

A. Graded Ca release. SR Ca release flux (black) tracks the amplitude of the L-type Ca current (red) during voltage clamps to different membrane voltages (V_m) in a rabbit ventricular myocyte [25], reproduced by the couplon network model(right). **B. Voltage-dependent EC coupling gain.** EC coupling gain, defined as the ratio of SR Ca release to the L-type Ca current amplitude, is higher at less depolarized voltages in experimental data from rabbit ventricular myocytes (left, from [25]). The steep decline in gain is reproduced better in the couplon network model(right) when the couplons are coupled (solid symbols) than when uncoupled (open symbols). **C. Steep SR fractional release-load relationship.** The fraction of SR Ca released increases steeply as the SR load increases in a rabbit ventricular myocyte [23] (left). The steepness is more accurately reproduced by the couplon network model(right) when the couplons are coupled (solid symbols) than when uncoupled (open symbols). **D. Ca alternans.** During rapid pacing with a fixed AP wavefrom (black), the Ca transient (red) alternates between large and small on successive beats in a patch-clamped rabbit ventricular myocyte (top panel), reproduced by the couplon network model[8](lower panels). 2nd panel shows alternans of the global Ca transient and SR Ca content during pacing with a fixed voltage waveform. 3rd and 4th panels show two representative couplons in the network, exhibiting irregular activations instead of alternans. 5th and 6th panels show the spatial patterns of Ca release from couplons during alternans on 4 successive beats. Note that when the two small beats or two large beats are compared to each other, the spatial patterns differ, indicating the macroscopic alternans is not accompanied by microscopic alternans.

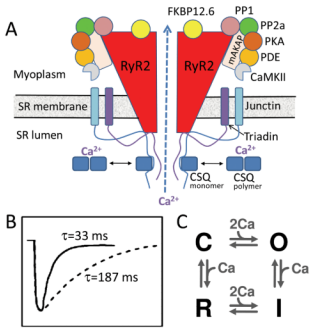

Fig. 4.

A. Ryanodine receptor macromolecular complex. The cardiac ryanodine receptor (RyR2) is a tetramer which forms a macromolecular complex with multiple interacting partners, including anchoring proteins (mAKAP + others not shown), protein kinases and phosphatases (PKA, CaMKII, PP1, PP2a), and other additional accessory regulatory proteins (FKBP12.6, triadin, junction, calsequestran, CSQ). **B. Couplon refractoriness.** Time course of SR refilling (solid line) vs couplon recovery from inactivation (dashed line), from Brochet et al [19]. **C. Simple four-state RyR model**, from Stern [24], without SR luminal Ca regulation.

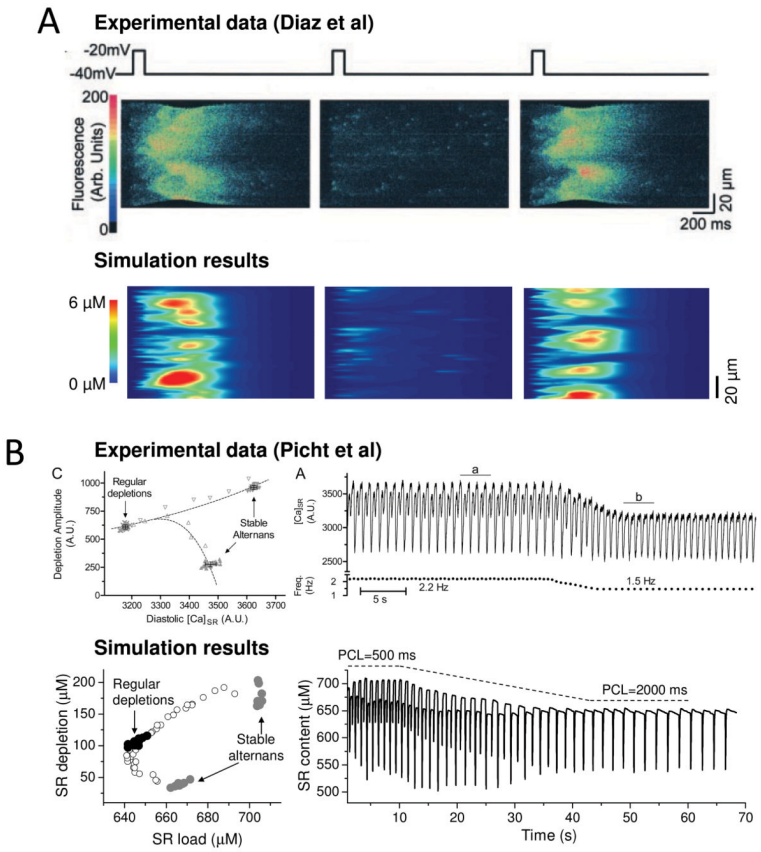

Fig. 5.

A. Ca alternans due to CICR waves on alternate beats, elicited by successive voltage clamp pulses from −40 to −20 mV in a ventricular myocyte (above, from [6]) and the couplon network model(below). Panels show line scans, with spatial position vertically and time horizontally. Note that the Ca waves initiate at different locations on the 1st and 3rd beats. **B. Dissociation between SR Ca release and load during alternans.** When heart rate was decreased (left panels) , Ca alternans resolved in a patch-clamped rabbit ventricular myocyte (above, from [32]) and the 3 R model [8] (below). Left panels show that SR load (diastolic $[Ca]_{SR}$) was lower during regular beating than during alternans, even though the SR depletion was larger than during the small Ca transient.

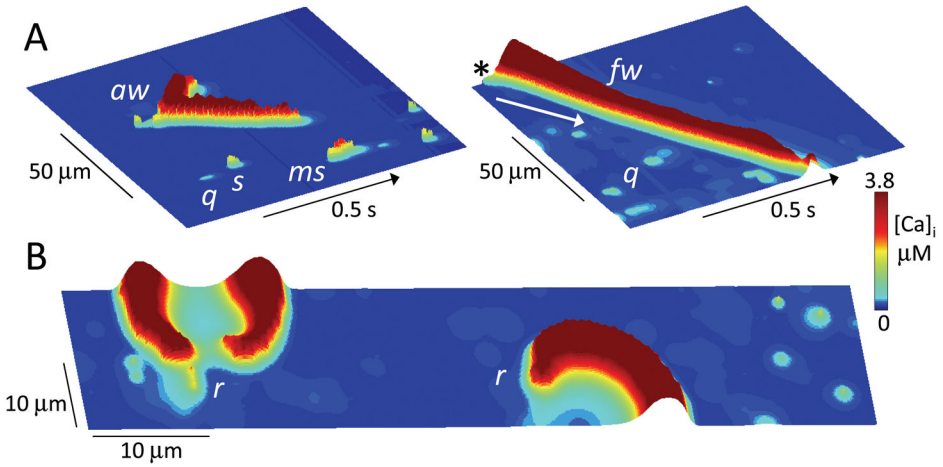

Fig. 6. Ca signaling hierarchy in the couplon network

A. Ca quarks (*q*), sparks (*s*), macrosparks (*ms*), aborted wave (*aw*) and full wave (*fw*), shown as labeled in line scans of cytoplasmic [Ca] along a line through the center of the couplon network array (100 x 20 µm) versus time. Cytoplasmic free [Ca] is indicated by height and color scale. In the right panel, the SR Ca load was higher to promote the full wave, which started as a spark in the upper corner (asterix) and propagated downward (arrow) by CICR through the full length of the couplon array. **B. Snapshot of Ca rotors (*r*)** in a couplon array (100 x 20 µm) at high SR Ca load. Figure-eight spiral wave reentry causing a double rotor is shown at left, with a single spiral wave rotor at right.

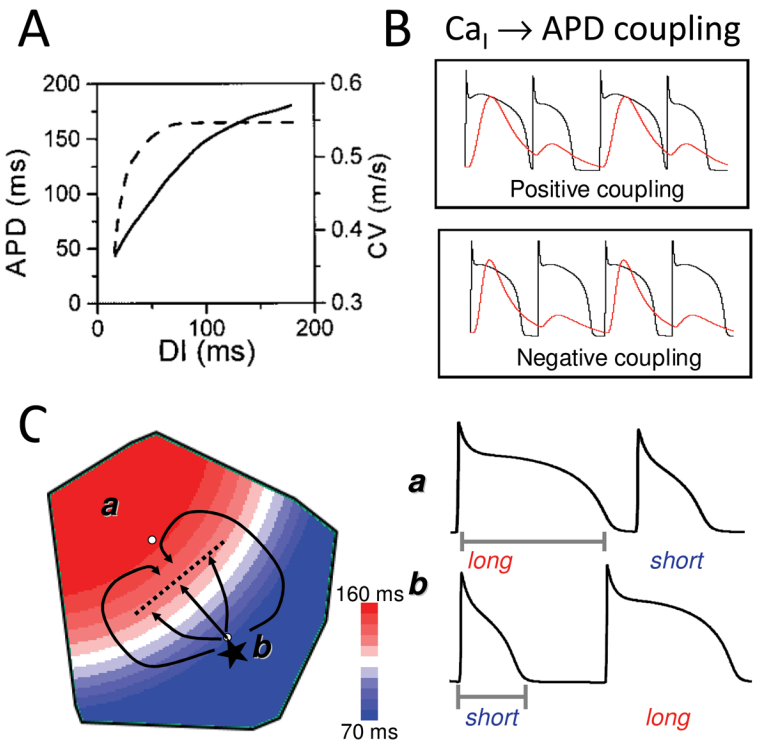

Fig. 7.

A. APD and CV restitution curves. As diastolic interval (DI) decreases, APD shortens and CV slows. **B. Positive and negative Ca_i-APD coupling.** See text. **C. Arrhythmogenic spatially discordant APD alternans.** In region A, APD alternans has a long-short pattern, whereas region B has a short-long pattern, separated by a nodal line without alternans. If a PVC (*) occurs in the short APD region, it can block as it propagates across the nodal line into in the long APD region, while propagating laterally until the long APD region recovers, initiating figure-eight reentry.

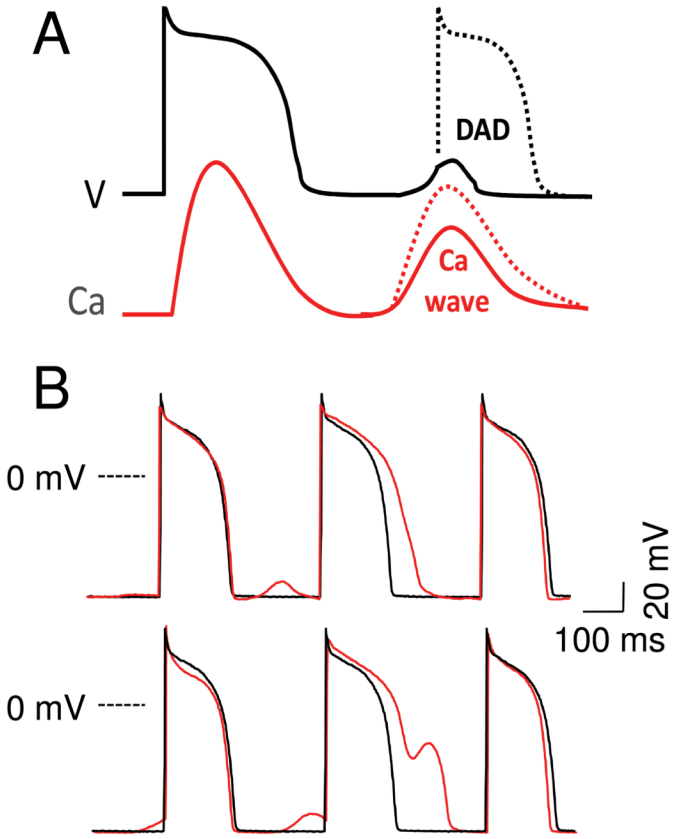

Fig. 8.

A. Sub- and supra-threshold DADs. Depending on the size and rate of rise of the Ca transient during the Ca wave(s), and the diastolic Ca-voltage coupling gain, a DAD can remain below or above the threshold to trigger an AP. **B. DAD-repolarization interaction.** DADs recorded from a paced isolated rabbit ventricular myocyte before (black traces) and after (red traces) exposure to isoproterenol. Depending on the timing, subthreshold DADs can cause APD prolongation (upper) and frank EADs (lower).